Pre-Clinical and Clinical Evaluation of Nuclear Tracers for the Molecular Imaging of Vulnerable Atheroclerosis : An Overview

Riou LM*, PhD [1, 2], Broisat A*, PhD [1, 2], Dimastromatteo J, MS [1, 2, 3], Pons G, MS [1, 2], Fagret D, MD, PhD [1, 2], Ghezzi C, PhD [1, 2]

[1]INSERM, U877, Radiopharmaceutiques Biocliniques, F-38000, Grenoble, France

[2] Université de Grenoble, F-38000, Grenoble, France

[3] ERAS Labo, F-38330, Saint Nazaire les Eymes, France

*LMR & AB equally contributed to this work.

Corresponding author:

Laurent M. Riou

INSERM, U877, Radiopharmaceutiques Biocliniques

Faculté de Médecine de Grenoble, F-38700, La tronche, France

Tel. +33(0)476 637 509 / Fax. +33(0)476 637 142

Running header: Nuclear tracers for vulnerable atherosclerosis imaging

ABSTRACT

Cardiovascular diseases (CVD) are the leading cause of mortality worldwide. Despite major advances in the treatment of CVD, a high proportion of CVD victims die suddenly while being apparently healthy, the great majority of these accidents being due to the rupture or erosion of a vulnerable coronary atherosclerotic plaque. A non-invasive imaging methodology allowing the early detection of vulnerable atherosclerotic plaques in selected individuals prior to the occurrence of any symptom would therefore be of great public health benefit.

Nuclear imaging could allow the identification of vulnerable patients by non-invasive in vivo scintigraphic imaging following administration of a radiolabeled tracer. The purpose of this review is to provide an overview of radiotracers that have been recently evaluated for the detection of vulnerable plaques together with the biological rationale that initiated their development. Radiotracers targeted at the inflammatory process seem particularly relevant and promising. Recently, macrophage targeting allowed the experimental in vivo detection of atherosclerosis using either SPECT or PET. A few tracers have also been evaluated clinically. Targeting of apoptosis and macrophage metabolism both allowed the imaging of vulnerable plaques in carotid vessels of patients. However, nuclear imaging of vulnerable plaques at the level of coronary arteries remains challenging, mostly because of their small size and their vicinity with unbound circulating tracer. The experimental and pilot clinical studies reviewed in the present paper represent a fundamental step prior to the evaluation of the efficacy of any selected tracer for the early, non-invasive detection of vulnerable patients.

Keywords: atherosclerosis / vulnerable coronary plaque / nuclear molecular imaging

Cardiovascular diseases (CVD) represent the leading cause of mortality worldwide. Coronary events are responsible for >50% of CVD deaths and for ~20% of deaths from all causes [1]. Rupture of a vulnerable coronary atherosclerotic plaque and subsequent thrombosis accounts for ~70% of coronary events [2]. The non-invasive detection of vulnerable atherosclerotic plaques responsible for the occurrence of a coronary event is therefore of great clinical relevance since it would allow the early identification and management of those patients at high cardiovascular risk [3].

Atherosclerosis is a chronic inflammatory disease in which oxidized Low Density Lipoproteins (oxLDL) initiate the inflammatory process at sites of endothelial dysfunction [2, 4-6]. Atherosclerotic plaques initially develop excentrically rather than concentrically [7], and non- or moderately obstructive plaques are responsible for the majority of acute coronary events [8]. An increased risk of coronary event is therefore not exclusively correlated with the degree of stenosis of any given plaque but also with the probability for a non-occlusive lesion to rupture or erode [3, 9]. Since coronary angiography only provides information about vessel lumen, non-obstructive vulnerable plaques cannot be detected using this technique. Imaging modalities such as intravascular ultrasound or optical coherence tomography are currently being evaluated for vulnerable plaque detection [10]. However, the invasive nature of these techniques limits their use to previously identified high-risk patients [11]. There is therefore a clinical need for a non-invasive molecular imaging modality allowing the screening of a large population for the detection of vulnerable coronary plaques. However, no such technique is currently available for routine clinical practice [12]. Among the various techniques that are currently being evaluated, nuclear imaging is a highly sensitive non-invasive imaging modality [13].

The recent development of high-resolution, high-sensitivity small animal dedicated imaging systems [14] has greatly helped for the pre-clinical in vivo evaluation of a number of new

potential tracers targeted at key steps of the atherogenic process leading to vulnerable plaques. The present paper will provide an overview of radiotracers that have been experimentally evaluated for Single Photon Emission Computed Tomography (SPECT) and Positron Emission Tomography (PET) imaging together with the biological rationales that justified their developments, with emphasis on the most promising agents.

Pathophysiology of Atherothrombosis

Depending on the stage of its development and on its constituents, atherosclerotic plaques are classified into six different categories according the American Heart Association (AHA) classification [15-17]. However, since the AHA classification was defined before the concept of vulnerable plaque emerged, further modifications have been proposed [18].

Initiation

Atherosclerotic lesions predominantly appear at sites of endothelial dysfunction, a phenomenon which in turn has been described at sites of arterial curvatures and bifurcations where low and oscillatory endothelial shear stress occurs [6, 19]. Under such conditions responsive elements are activated, leading to endothelial gene expression responsible for a large spectrum of modifications among which intimal thickening, defined as the proliferation of SMCs in the intima, and decreased nitric oxide (NO) synthesis. Not only is NO a key regulator of vascular tone but it also is a powerful anti-inflammatory, anti-mitotic and anti-thrombotic compound [20]. In addition, endothelial dysfunction is characterized by increased reactive oxygen species (ROS) production. The increased endothelial permeability together with ROS production are responsible for the accumulation of immunogenic oxLDL in the subendothelial space. Moreover, activation of the transcriptional nuclear factor NFKB leads to

the activation of multiple pro-immunogenic genes whose products are involved in the recruitment of leucocytes [21]. Adhesion molecules, such as the E-selectin and the intercellular and vascular adhesion molecules ICAM-1 and VCAM-1, as well as the chemokines monocyte chemoattractant protein-1 (MCP-1) and interleukin 8 (IL-8) are involved in the recruitment of circulating monocytes and lymphocytes into the arterial wall [22, 23]. Macrophage Colony Stimulating Factor (MCSF) induces the differentiation of recruited monocytes into macrophages. These activated macrophages express the scavenger receptors SR-A, CD36 and LOX-1 on their surface [24-26]. These receptors are involved in the recognition and uptake of oxLDL. Ultimately, the intracytoplasmic accumulation of lipid droplets within macrophages results in the formation of foam cells. Moreover, Lectin-like OxLDL receptor-1 (LOX-1) is also expressed by the endothelium, smooth muscle cells (SMC) and platelets, and oxLDL binding to LOX-1 leads to intracellular signaling resulting in ROS- and NFKB-induced endothelial dysfunction as well as in apoptosis [26]. In addition to scavenger receptors, it has been proposed that another class of immune receptors, the toll-like receptors (TLRs), may play a role in the initiation and progression of the atherosclerotic lesions. TLRs recognize a number of pathogens as well as endogenous molecules involved in the onset of atherosclerosis (necrotic cells, heat shock proteins, fibronectin) and their stimulation results in the activation of NFKB and various cytokines [27, 28].

According to the AHA classification, type I lesions consist in isolated macrophage-derived foam cells that contain lipid droplets whereas type II lesions contain numerous macrophage foam cells. Finally, type III lesions are characterized by extracellular lipid deposit [15-17].

Advanced Atherosclerotic Plaques

Macrophages and foam cells synthetize pro-inflammatory cytokines such as MCP-1. In addition, macrophages interact with T1 and T2 lymphocytes [4, 29]. The interaction between

CD40 and its ligand CD40L plays a major role in the interaction between macrophages and lymphocytes, as well as between those inflammatory cells and SMCs [30, 31]. As a result, the immune response is greatly amplified. Among the various cytokines synthesized at this stage of atherosclerosis development, interferon-gamma (IFNγ) stimulates the proliferation of SMCs already present in areas of intimal thickening. In order for macrophages, lymphocytes and SMCs to migrate within the intima and media, these cells release metalloproteinases (MMPs) that digest the extracellular matrix (collagenase, gelatinases, elastases and stromelysins) [32, 33]. Those three cell types also produce tissue factor, a small pro-thrombotic compound that plays a major role in thrombus formation when exposed to the blood stream at the time of plaque rupture [34]. Macrophage- and SMC-derived foam cells eventually undergo apoptosis as a result of intracellular oxLDL toxicity and therefore participate to the formation of an acellular lipidic and necrotic core [29, 35]. SMCs exert different roles in advanced atherosclerotic plaques. On one hand and as mentioned above, SMCs produce MMPs and ingest oxLDL, thereby participating in plaque destabilisation and to foam cell formation. On the other hand, SMCs synthesize the fibrous cap that covers the lipidic and necrotic core, therefore stabilizing the plaque [36, 37]. It has become clear that the cellular and extracellular composition of the plaque represent a primary determinant of plaque stability. Prone-to-rupture vulnerable plaques are characterized by a large lipidic and necrotic core (>40%) covered by a fine fibrous cap (<65μm) and by intense inflammatory processes whereas more stable plaques are characterized by a minimal lipidic and necrotic core and a thick fibrous or calcified cap [3, 9]. Because of arterial wall remodeling, blood diffusion from the arterial lumen or blood supply from the preexisting vaso vasorum is no longer sufficient and angiogenesis is necessary. Neovessels originate from the existing vasa vasorum in the adventitia and extend within the atherosclerotic lesion in the media. Angiogenesis participates in lesion development by extracellular matrix destabilisation as well as by acting as a pathway

for LDL diffusion, mononuclear leucocytes recruitment, and red blood cell extravasation [38-40].

AHA type IV lesions are characterized by a large lipidic and necrotic core resulting from the fusion of droplets observed in type III plaques. Type Va lesions are characterized by a large lipidic and necrotic core covered by a fibrous cap. Calcified type V plaques are called Vb whereas type V plaques with minimal lipidic and necrotic core and extensive fibrosis are classified as Vc. Type V plaques might become occlusive and cause unstable angina. There is no specific category for the vulnerable thin cap fibroatheroma. This type of vulnerable plaque belongs either to type IV or V lesion [15-17].

Thrombus Formation

Following plaque rupture, a number of thrombogenic factors influence the magnitude and stability of the thrombus and therefore the development of atherosclerotic lesions and the clinical severity of the coronary syndrome. In order to take into account the key role of thrombosis, the concepts of atherosclerosis and thrombosis have therefore been unified in the term atherothrombosis [2].

In approximately two third of the cases, thrombus formation occurs at the site of plaque rupture, the remaining thrombotic events being due to erosion of a vulnerable plaque [41]. The combination of weak plaque composition as usually observed at the shoulder of plaques (i.e. thin fibrous cap, intensive macrophages infiltration, matrix degradation and apoptosis) with an increase in the external circumferential and shear stresses are held responsible for the rupture of vulnerable plaques. The amplitude of thrombus formation depends on various factors including the rheology and the concentration of pro-thrombotic factors present within the ruptured exposed plaque as well as in the blood [2]. The thrombus might be occlusive or

not, and might cause clinical symptoms. Acute occlusion at the site of plaque rupture or downstream can be responsible for myocardial infarction.

Complicated Atherosclerotic Plaques

Finally, AHA type VI atherosclerotic lesions result from the complication of type IV or type Va lesions following plaque rupture/erosion or intra-plaque haemorrhage [15-17]. Following culprit lesion healing and thrombus inclusion, the plaque might then evolve into a fibrous and potentially stenotic lesion. Alternatively, new episodes of rupture and thrombus formation can also occur.

Nuclear Imaging of Vulnerable Plaques

The non-invasive imaging modalities currently under evaluation for the detection of vulnerable plaques can be divided into morphologic techniques such as magnetic resonance or computed tomography, and molecular imaging techniques such as nuclear medicine or ultrasound. While exquisite resolution is required for morphologic techniques, the very high sensitivity of molecular nuclear imaging allows to distinguish a vulnerable from a stable plaque based on the detection of a specific molecular target. Potential radiotracers for the molecular imaging of vulnerable atherosclerosis are compounds targeted at key molecules or processes involved in atherogenesis. Such agents are radiolabeled either with γ- or β^+-emitters, allowing the non-invasive imaging of their biodistribution using either SPECT or PET cameras, respectively. A brief overview of the radiotracers that have been evaluated so far for the detection of atherosclerotic lesions is provided in Table 1.

Table 1. Summary of previously evaluated radiotracers for the nuclear detection of atherosclerotic lesions.

Target	Tracer	Nature of tracer	Model	Lesion location	Assessment of tracer uptake	Reference
LDL	[^{125}I]-LDL	Lipoprotein	Humans	Carotid	In vivo imaging	[42]
			NZW Rabbits	Aorta	Ex vivo biodistribtion	[48]
	[^{99m}Tc]-LDL	Lipoprotein	Humans	Carotid	In vivo imaging	[45]
			NZW Rabbits	Aorta	In vivo imaging	[43]
	[^{123}I]-LDL	Lipoprotein	NZW Rabbits	Aorta	In vivo imaging	[49]
	[^{111}In]-LDL	Lipoprotein	NZW Rabbits	Aorta	Ex vivo biodistribution	[46]
OxLDL	[^{99m}Tc]-oxLDL	Lipoprotein	Humans	Carotid	In vivo imaging	[50]
	[^{123}I]-SP4	Oligopeptide	WHHL Rabbits	Aorta	In vivo imaging	[51]
	[^{99m}Tc]-P199	Oligopeptide	WHHL Rabbits	Aorta/carotid	Ex vivo imaging	[52]
	[^{125}I]-MDA2	Antibody	LDLR$^{-/-}$ mice/WHHL Rabbits	Aorta	Ex vivo imaging	[54]
			LDLR$^{-/-}$ mice	Aorta	Ex vivo imaging	[55]
	[^{99m}Tc]-MDA2	Antibody	WHHL Rabbits	Aorta	In vivo imaging	[53]
	[^{125}I]-IK17	Antibody	LDLR$^{-/-}$ mice	Aorta	Ex vivo imaging	[56]
	[^{124}I]-CD68Fc	Peptide	ApoE$^{-/-}$ mice	Aorta	Ex vivo imaging	[58]
LOX-1	[^{99m}Tc]-LOX1-mAb	Antibody	WHHLMI Rabbits	Aorta	In vivo imaging	[61]
Monocyte/macrophage CCR-2	[^{125}I]-MCP-1	Peptide	NZW Rabbits	Aorta	Ex vivo imaging	[62]
	[^{99m}Tc]-MCP-1	Peptide	NZW Rabbits	Aorta	In vivo imaging	[63]
Macrophage metabolism	[^{18}F]-FDG	Carbohydrate	Humans	Carotid/Aorta	In vivo imaging	[64, 65]
			Humans	Carotid	In vivo imaging	[68]
			Humans	Carotid/Aorta	In vivo imaging	[70-72]
			WHHL/WHHLMI/NZW rabbits	Aorta	In vivo imaging	[66, 73]
			NZW rabbits	Aorta	In vivo imaging	[67]
			NZW rabbits	Aorta	In vivo imaging	[69]
			ApoE$^{-/-}$ mice	Aorta	No tracer accumulation in lesions	[74]
	[^{18}F]-Choline	Amino alcohol	ApoE$^{-/-}$ mice	Aorta	Ex vivo imaging	[85]
Monocyte/macrophage	[^{111}In]-monocytes	Cells	ApoE$^{-/-}$ mice	Aorta	In vivo imaging	[86]
	[^{64}Cu]-TNP	Nanoparticle	ApoE$^{-/-}$ mice	Aorta	In vivo imaging	[87]
VCAM-1	[^{99m}Tc]-B2702p	Peptide	WHHL Rabbits	Aorta	Ex vivo imaging	[92]
	[^{99m}Tc]-B2702p der.	Peptide	ApoE$^{-/-}$ mice	Carotid	In vivo imaging	[94]
MMPs	[^{123}I]-HO-CGS27023A	Hydroxamate der.	ApoE$^{-/-}$ mice	Carotid	In vivo imaging	[96]
Apoptosis	[^{99m}Tc]-Annexin A5	Protein	NZW Rabbits	Aorta	In vivo imaging	[100, 104, 105]
			WHHLMI Rabbits	Aorta	In vivo imaging	[101]
			Swine	Coronary	In vivo imaging	[102]
			ApoE$^{-/-}$ / LDLR$^{-/-}$ mice	Aorta	In vivo imaging	[103]
			ApoE$^{-/-}$ mice	Aorta	Ex vivo imaging	[106]
			Humans	Carotid	In vivo imaging	[108]
	[^{99m}Tc]-Ap$_4$A	Purine analog	NZW Rabbits	Aorta	In vivo imaging	[109]
Angiogenesis / $\alpha_v\beta_3$ integrin	[^{111}In]-RP748	peptidomimetic	ApoE$^{-/-}$ mice	Carotid	Ex vivo imaging	[117]
Angiogenesis / ED-B	[^{125}I]-L19	Antibody	ApoE$^{-/-}$ mice	Aorta	Ex vivo imaging	[118]
Angioenesis / Tenascin C	[^{125}I]-G11	Antibody	ApoE$^{-/-}$	Aorta	Ex vivo imaging	[119]
Oncogene activation	[^{99m}Tc]-ASONs	Antisense nucleotide	NZW rabbits	Aorta	In vivo imaging	[122]

NZW, New Zealand White; WHHL, Watanabe Heritable Hyperlipidemic; WHHLMI, WHHL Myocardial Infarction-prone; der., derivative

Low Density Lipoprotein Imaging

Countless studies indicated that native LDLs and oxLDLs play a critical role in the pathogenesis of unstable atherosclerosis [4]. Different strategies have therefore been used to image LDL accumulation into atherosclerotic lesions. Direct radiolabeling of LDLs was performed using ^{125}I, ^{99m}Tc, ^{123}I, and ^{111}In [42-49]. In a clinical study, Lees et al. [45] observed focal accumulation of [^{99m}Tc]-LDL in the carotid, iliac, and femoral vessels of 4 / 17 patients with atherosclerosis. However, the slow kinetics of LDL accumulation together with the high circulating tracer activity precluded in vivo image acquisition. As oxLDLs are predominantly implicated in the processes leading to vulnerable plaque formation, some authors performed in vitro oxidation of native LDLs with copper and hydrogen peroxide prior to radiolabeling using ^{99m}Tc [50]. [^{99m}Tc]-oxLDLs demonstrated better tissue accumulation and more favorable blood kinetics than radiolabeled native LDL. In 7 patients with transient ischemic attacks, [^{99m}Tc]-oxLDLs allowed carotid plaque imaging in 10 out of 11 lesions with target-to-background ratios of ~1.5 [50]. Hardoff et al. have attempted in vivo imaging of aortic atherosclerosis in Watanabe Heritable Hyper-Lipidemic (WHHL) rabbits with a radiolabeled synthetic oligopeptide fragment of apolipoprotein B, SP-4 [51, 52]. Although [^{123}I]-labeled SP-4 allowed the non-invasive detection of atherosclerotic lesions in 12 out of 14 WHHL animals, radiolabeling of SP-4 with the more suitable isotope ^{99m}Tc yielded mixed results with only weak focal aortic uptake of [^{99m}Tc]-SP-4 in 8 out of 11 hyperchoelsterolemic rabbits. An alternative strategy to image oxLDL accumulation into atherosclerotic plaques was employed by Tsimikas et al. [53]. The authors demonstrated that intravenously injected, radiolabeled oxidation-specific antibodies (Ox-AB), such as the murine monoclonal antibody (mAb) MDA2, which detects malondialdehyde (MDA)–lysine epitopes, have a strong and specific predilection for atherosclerotic lesions but not for normal arteries. Aortic uptake of [^{125}I]-MDA2 was enhanced in lipid-rich lesions of LDLR$^{-/-}$ mice fed a western-type diet

whereas it was reduced in the lesions of animals on antioxidant diets [54]. [^{99m}Tc]-labeled MDA2 allowed the non-invasive imaging of atherosclerotic lesions in 4 out of 7 WHHL rabbits [53, 55]. However, the slow blood kinetics of radiolabeled MDA2 required an extensive period of time between tracer injection and image acquisition together with the injection of MDA-LDL in order to minimize the radiolabeled MDA2 circulating activity. The phage display method has also been used to identify human monoclonal antibodies against oxidation-specific epitopes of oxLDL. Various sequences have been described, among which IK17 specifically bound MDA-LDL, intact oxLDL but not native LDL. Intravenous injection of [^{125}I]-IK17 into hypercholesterolemic LDLR$^{-/-}$ mice resulted in specific uptake of the tracer in aortic atherosclerotic lesions [56, 57]. However, the feasibility of non-invasive imaging of atherosclerotic lesions using [^{125}I]-IK 17 has not been demonstrated so far. Preliminary data from Langer et al. recently suggested that the conjugation of the soluble dimeric form of the scavenger receptor CD68 to a human Fc-fragment could be used to perform autoradiographic imaging of oxLDL accumulation in atherosclerotic lesions from hypercholestrolemic ApoE$^{-/-}$ mice following radiolabeling with the PET-suitable isotope ^{124}I [58].

LOX-1 is a scavenger receptor expressed by endothelial cells, monocytes, macrophages, smooth muscle cells, and platelets which displays picomolar affinity for oxLDL. The role of LOX-1 in the initiation, progression, and destabilization of atherosclerotic plaques has been recently described [59, 26]. In human carotid atherosclerotic lesions, LOX-1 expression has been observed in luminal endothelial cells from early atherosclerotic lesions as well as in intimal endothelial cells from the neovasculature and in macrophages and smooth muscle cells from advanced atherosclerotic lesions [60]. As shown in Fig. (**1**), Ishino S. et al [61] recently described the experimental evaluation of a ^{99m}Tc-labeled anti–LOX-1 monoclonal IgG ([^{99m}Tc]-LOX-1-mAb) for the non-invasive planar imaging of atherosclerosis in myocardial infarction–prone Watanabe heritable hyperlipidemic [WHHLMI] rabbits. The

authors showed that despite a poor correlation between tracer activity and LOX-1-expressing macrophages on autoradiographic and immunohistologic images, respectively, [^{99m}Tc]-LOX-1-mAb allowed the non-invasive planar imaging of atherosclerosis at 24 hours following intravenous injection with robust differential uptake ratios (DURs). [^{99m}Tc]-LOX-1-mAb DURs were 2.4- and 3.2-fold higher than [^{18}F]-FDG DURs in the thoracic and abdominal aortic segments of WHHL rabbits, respectively [62], and 5.7- and 3.7-fold higher than [^{99m}Tc]-Annexin A5 DURs in the thoracic and abdominal aortic segments of WHHLMI rabbits, respectively [63]. However, as usually observed when evaluating radiolabeled antibodies, high levels of circulating tracer probably accounted for the relatively low lesion-to-blood ratios, which might be improved by evaluating alternative strategies aimed at accelerating [^{99m}Tc]-LOX-1-mAb blood clearance.

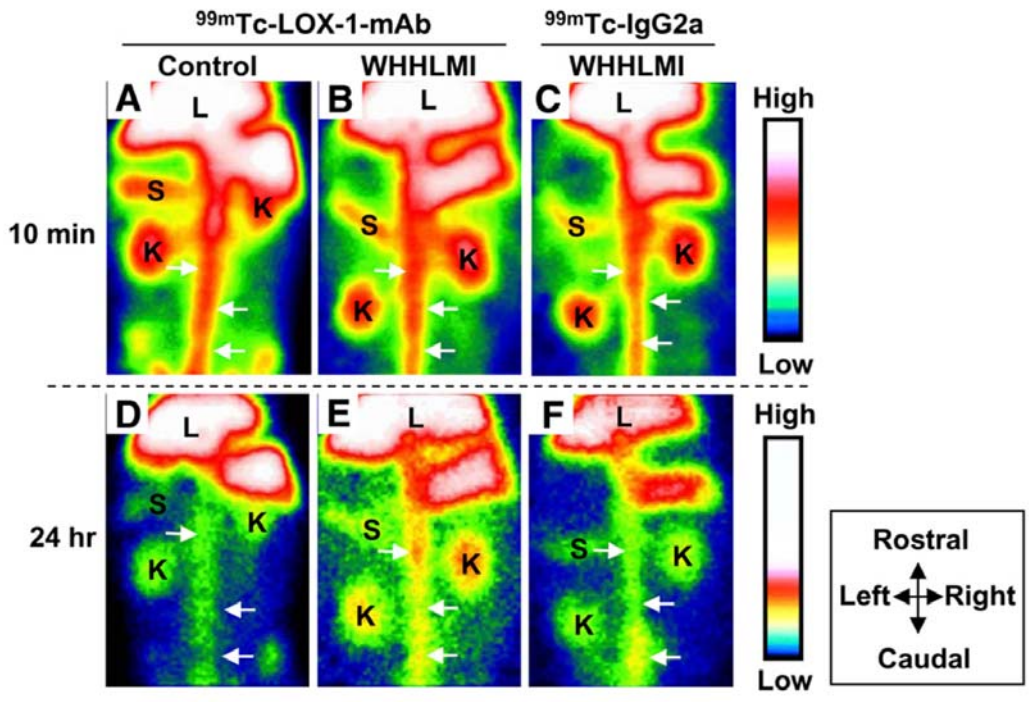

Fig (**1**). Non-invasive in vivo planar imaging of lectin-like oxLDL receptor-1 (LOX-1) with [^{99m}Tc]-LOX-1-mAb. Non-invasive imaging of abdominal region with [^{99m}Tc]-LOX-1-mAb (A, B, D, and E) and [^{99m}Tc]-IgG2a (C and F). Planar images for WHHLMI (B, C, E, and F) and control (A and D) rabbits at 10 min (A–C) and 24 hours (D–F) after injection are shown. Field of view = 170 x 120 mm. Arrows = aorta; K = kidney; L = liver; S = spleen. Reproduced from [61] with permission from the Society of Nuclear Medicine.

Inflammation Imaging

Monocyte Chemoattractant Protein-1 (MCP-1)

Circulating monocytes are attracted to the site of atherosclerotic plaque development by MCP-1, a chemokine which is produced by endothelial cells, smooth muscle cells and monocytes/macrophages over the course of atherosclerotic plaque formation. MCP-1 binds to the CCR-2 receptor on the cellular membrane of monocytes / macrophages [22]. ^{125}I-radiolabeled MCP-1 has therefore been evaluated for the molecular imaging of atherosclerotic plaque following injection into hypercholesterolemic rabbits with arterial injury-induced atherosclerotic lesions. A fast blood clearance was observed with a halflife of ~10 minutes. Although in vivo imaging was not attempted due to the suboptimal image quality obtained when using ^{125}I-labeled tracers, autoradiograms revealed [^{125}I]-MCP-1 accumulation in the damaged artery wall which was correlated with the number of infiltrated macrophages [64]. MCP-1 has been recently radiolabelled with ^{99m}Tc and injected into rabbits with atherosclerotic lesion induced by balloon deendothelialization of the abdominal aorta [65]. Ex vivo imaging indicated that [^{99m}Tc]-MCP-1 uptake in atherosclerotic lesions was 4-fold higher than that observed in the vessels of control animals. A strong correlation between [^{99m}Tc]-MCP-1 and macrophage density was also observed, and tracer uptake was detected at the lesion site by non-invasive in vivo imaging as shown in Fig. (**2**). [^{99m}Tc]-labeled MCP-1 is therefore a promising agent for the molecular imaging of vulnerable atherosclerotic plaques.

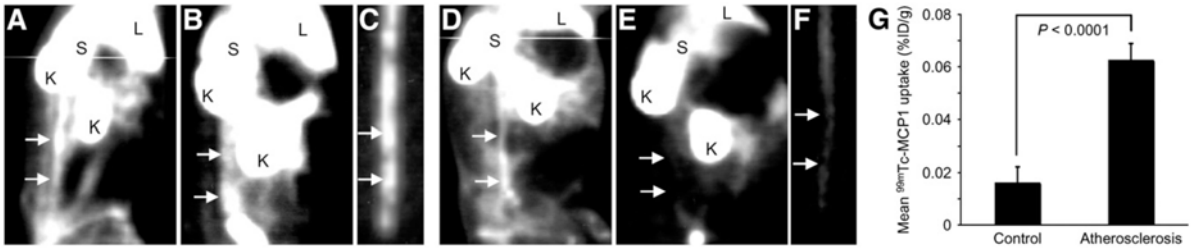

Fig (**2**).Non-invasive in vivo planar imaging of macrophage CCR-2 receptors with [^{99m}Tc]-MCP-1. Images were obtained in both New Zealand White (NZW) rabbits submited to deendothelialization of the abdominal aorta and fed a high-cholesterol diet (atherosclerotic, [A-C]) and control, unmanipulated, NZW animals fed normal rabbit chow (non-atherosclerotic, [D-F]) rabbits. (A-C) Planar γ-images of atherosclerotic rabbit. (A) Image obtained immediately after intravenous [^{99m}Tc]-MCP-1 administration outlines aortic blood-pool activity (arrows). (B) At 3 hours after radiotracer administration, significant radiotracer accumulation is evident in abdominal aorta (arrows). (C) Ex vivo image of explanted aorta confirms in vivo evidence of [^{99m}Tc]-MCP-1 uptake (arrows). (D-F) Planar γ-images of control rabbit. (D) Aortic blood pool is seen at time of intravenous [^{99m}Tc]-MCP-1 injection (arrows). (E) Image shows lack of [^{99m}Tc]-MCP-1 uptake in region of abdominal aorta, as denoted by arrows in normal rabbit with no atherosclerotic lesions. (F) Ex vivo aortic image of control animal demonstrates absence of [^{99m}Tc]-MCP-1 uptake (arrows). L = liver; S = spleen; K = kidney. (G) Bar graphs show quantitative [^{99m}Tc]-MCP-1 uptake within abdominal aortas of atherosclerotic and control animals represented as mean %ID/g ± SD. [^{99m}Tc]-MCP-1 uptake (%ID/g) was significantly higher in atherosclerotic animals (P<0.0001) compared with that of control animals. Reproduced from [65] with permission from the Society of Nuclear Medicine.

[^{18}F]-FDG

Atherosclerotic plaque inflammation was imaged in patients with symptomatic carotid atherosclerosis using the glucose analog [^{18}F]-FDG by Rudd et al. [66], and the authors recently demonstrated the reproducibility of the methodology [67]. [^{18}F]-FDG accumulated into macrophage-rich areas of the plaque, and symptomatic, unstable plaques accumulated more [^{18}F]-FDG than did asymptomatic lesions. Experimental and clinical studies have since then confirmed that the vascular uptake of the tracer is correlated with macrophage content, but not with smooth muscle cells or vascular wall thickness, and that the most likely mechanism for [^{18}F]-FDG accumulation into infiltrated macrophages is the high glucose metabolism of macrophages under pro-inflammatory conditions such as those encountered in vulnerable atherosclerotic plaques [62,68-70]. A representative example of in vivo experimental atherosclerotic plaque imaging with [^{18}F]-FDG is shown in Fig. (**3**).

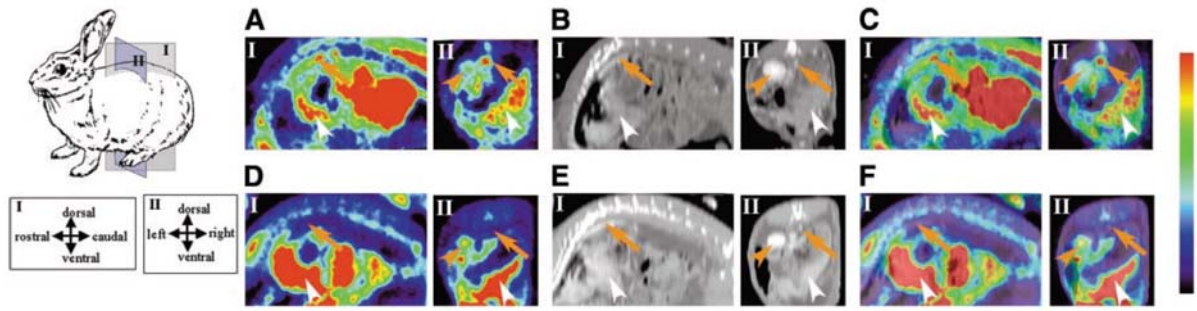

Fig (**3**).Non-invasive in vivo PET imaging of macrophage metabolism using [^{18}F]-FDG. PET images (A and D), CT images (B and E), and superimposed PET/CT images (C and F) in the sagittal (I) and coronal (II) planes for WHHL (A, B, and C) and control (D, E, and F) rabbits. Orange arrows, orange arrowheads, and white arrowheads indicate aortas, kidneys, and livers, respectively. Reproduced from [62] with permission from the Society of Nuclear Medicine.

Based on these studies, [^{18}F]-FDG has been used to evaluate the prevalence of inflammation in documented carotid atherosclerosis [71], and Tahara et al. [72] recently suggested that the metabolic syndrome was associated with increased [^{18}F]-FDG uptake, and therefore increased inflammation, in carotid atherosclerosis. [^{18}F]-FDG has also been successfully used to monitor the effect of lipid-lowering and anti-oxidant treatments on plaque inflammation [73, 74]. The only controversial study with regards to [^{18}F]-FDG uptake in atherosclerotic plaque was that of Laurberg et al [75]. The authors did not observe increased aortic and carotid tracer accumulation in hypercholesterolemic, apoE$^{-/-}$ mice neither by in vivo PET imaging nor by γ-well counting of excised vessels. The discrepancy between the results of this study and others remains unexplained [76]. Strong evidence is therefore now available to suggest that [^{18}F]-FDG carotid imaging is a sensitive and reproducible method for the detection of plaque inflammation. However, a potential limitation of coronary atherosclerotic plaque imaging with [^{18}F]-FDG is the high myocardial background uptake of the tracer which might hamper the signal-to-background ratio. Positron-sensitive probes are being evaluated in the setting of phantom, ex vivo, or in vivo studies. Although tracer detection would now be performed invasively, initial results suggested the feasibility of intravascular [^{18}F]-FDG detection in vessels ≥1 mm in diameter [77-81].

[^{18}F]-Choline

[^{18}F]-Choline was initially introduced as a tracer for brain and prostate cancer imaging [82]. Choline is taken up into cells by specific transport mechanisms, phosphorylated by choline kinase, metabolized into phosphatidylcholine, and eventually incorporated into the cell membrane. Increased choline uptake has been observed in activated macrophages [83], and a correlation was observed between [^{18}F]-Choline uptake and macrophage accumulation in experimental models of soft tissue infection [84] and acute cerebral radiation injury [85]. Matter et al. [86] have therefore investigated the potential of [^{18}F]-Choline for the molecular imaging of atherosclerotic plaque. Using ex vivo imaging, [^{18}F]-Choline uptake correlated better with lipid-positive and macrophage-positive areas than [^{14}C]-FDG in hypercholesterolemic, ApoE$^{-/-}$ mice [86]. However, PET imaging failed to detect [^{18}F]-Choline uptake in atherosclerotic lesions in vivo. Further studies are therefore warranted to clarify the potential of [^{18}F]-Choline for the in vivo imaging of macrophage accumulation in atherosclerotic plaques.

Monocytes / Macrophages Cellular Imaging

Two recent studies focused on monocyte / macrophage cellular imaging. First, Kircher et al. [87] performed in vitro ^{111}In-Oxine monocytes labeling prior to reinjection of radiolabeled cells into apoE$^{-/-}$ or control mice in order to gain insights into the pathogenesis of atherosclerosis. Five days following injection, monocyte recruitment to plaques could be assessed by micro-SPECT/CT imaging and visualized as a focal hotspot in the ascending aorta with good correlation between the in vivo SPECT signal and the monocyte content (R^2 = 0.87). The inhibition of monocyte recruitment following statin treatment was also evidenced using this methodology. Clinical studies are now warranted, especially considering the fact that ^{111}In-oxine is approved by the Food and Drug Administration for clinical use.

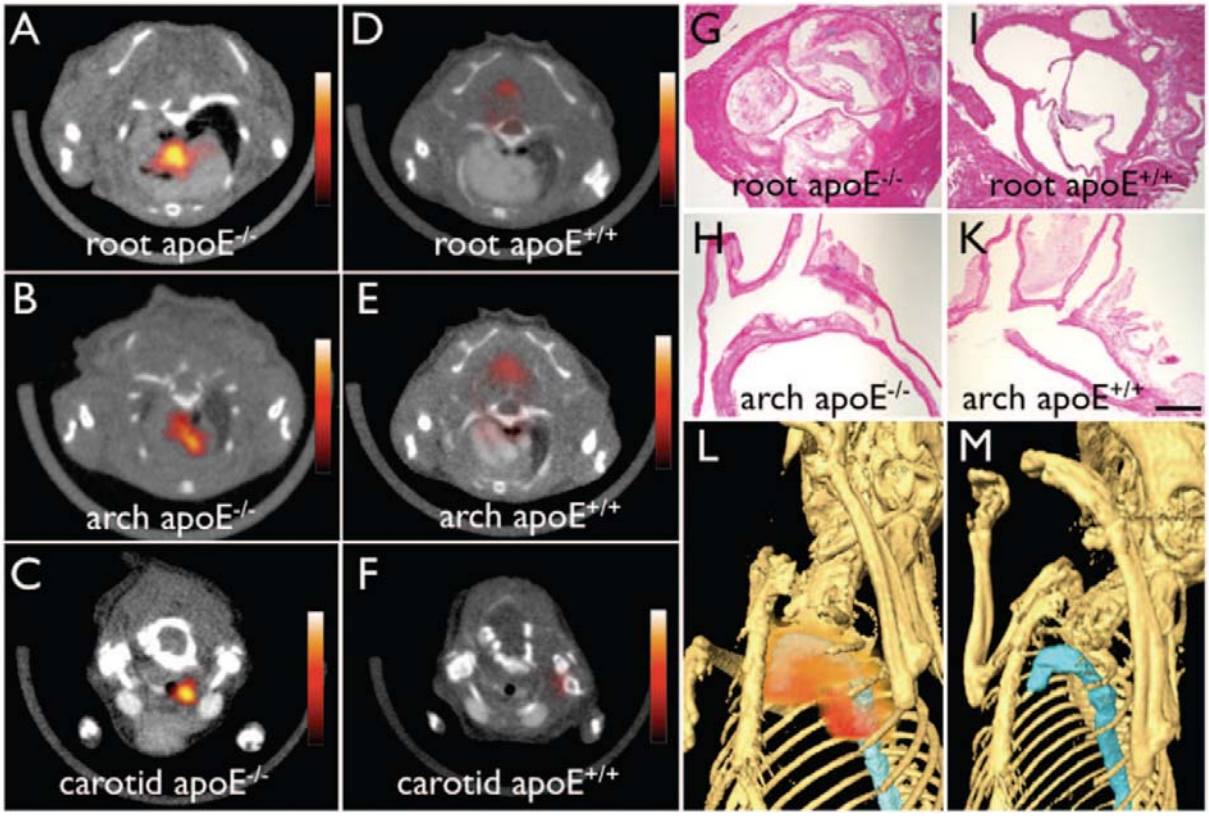

Fig (**4**).Non-invasive in vivo PET imaging of macrophages with a ^{64}Cu-labeled trireporter nanoparticle [^{64}Cu]-TNP. [^{64}Cu]-TNP facilitates PET-CT imaging of inflammatory atherosclerosis in apoE$^{-/-}$ mice. Fused PET-CT images of the aortic root (A), arch (B), and carotid artery (C) of aged apoE$^{-/-}$ mice show strong PET signal in these vascular territories with high plaque burden, whereas no activity is observed in the same vasculature of wildtype mice (D through F). G and H, Hematoxylin and eosin histology of respective vascular regions, which carry a high plaque burden in apoE$^{-/-}$ but not in wild-type mice (I through K) (magnification: x 400 for G and I, x200 for H and K; bar=0.4 mm). The 3-dimensional maximum intensity reconstruction of the fused data set (L) demonstrates focal PET signal (red) in the proximal thoracic aorta (blue) of an apoE$^{-/-}$ mouse but not in a wild-type mouse (M). Reproduced from [88] with pending permission from the American Heart Association.

Second, based on the concept that macrophages are avid for polysaccharide-containing supramolecular structures such as nanoparticules, a dextranated and DTPA-modified magnetofluorescent 20-nm nanoparticle was recently labeled with the PET tracer ^{64}Cu ([^{64}Cu]-TNP) to yield a PET, magnetic resonance, and optically detectable imaging agent which provided nuclear images of aortic atherosclerotic plaques 24 hours following injection in ApoE$^{-/-}$ mice [88] as shown in Fig. (**4**).

Vascular Cell Adhesion Molecule -1 (VCAM-1)

Endothelial cells express specific molecules when subjected to pro-atherogenic conditions [22]. Among those, VCAM-1 plays a major role in the recruitment of inflammatory cells such as monocytes and lymphocytes to developing atherosclerotic plaques [23]. In advanced lesions, VCAM-1 is also expressed at the level of neovessels as well as by SMCs and macrophages from the media [38].

To date, a few studies have addressed the use of VCAM-1 as a target for the molecular imaging of vulnerable plaques. Using intravascular ultrasound and echogenic immunoliposomes (ELIPSs) targeted at VCAM-1, Hamilton and colleagues demonstrated a significant increase in mean gray scale values on endothelial images of injured carotid arteries from Yucatan miniswines when compared to images obtained with non-specific ELIPs [89]. More recently, in vitro phage display was used by Kelly et al. to select a VCAM-1 specific peptide sequence that was used for the production of magnetofluorescent nanoparticles [90]. Although ex vivo images of VCAM-1 expression were performed, this agent turned out to be suboptimal for in vivo imaging. Using in vivo phage display in apoE$^{-/-}$ mice, the authors then described a peptide sequence highly homologous to the known VCAM-1 ligand VLA-4 which displayed an improved affinity for VCAM-1. This peptide was used for the production of a second-generation agent detectable through MRI and optical imaging which provided very promising results with respect to the in vivo imaging of variable levels of VCAM-1 expression [91]. Finally, Kaufmann et al. recently described the feasibility of the in vivo monitoring of VCAM-1 aortic expression of control and hypercholesterolemic mice fed normal or high-fat diets using contrast echocardiography and VCAM-1-targeted microbubbles [92].

We recently described the ex vivo imaging of VCAM-1 expression in hypercholesterolemic rabbits using a ^{99m}Tc-labeled version of the HLA class I-derived peptide B2702 [93] that was

previously shown to bind specifically to VCAM-1 [93]. Moreover, in vivo imaging of VCAM-1 expression in a mouse model of atherosclerotic plaque development induced by left carotid artery ligation in apoE$^{-/-}$ animals was performed using a peptidic derivative of [^{99m}Tc]-B2702 [95].

Matrix Metalloproteinases (MMPs) Imaging

MMPs are involved in the remodeling of connective tissue. In the setting of atherogenesis, MMPs are secreted by various cell types [32, 33]. Macrophages represent the predominant source of MMPs over the course of vulnerable plaque development. MMP inhibitors (MMPIs) bind to MMPs with high affinity. Several hydroxamate-derivatives with MMP inhibitory properties in the nanomolar range have been synthetized (HO-CGS 27023A 1a-1i) and radiolabelled using iodine-123 ([^{123}I]-HO-CGS 27023A 1a-1i) in order to evaluate their potential for the molecular imaging of atherosclerotic plaques [96]. [^{123}I]-HO-CGS 27023A has been injected in an experimental mouse model of carotid arterial remodeling induced by carotid artery ligation and characterized by macrophage infiltration and MMP overexpression. [^{123}I]-HO-CGS 27023A in vivo accumulation in the carotid lesion was inhibited by pretreatment with an excess of unlabeled compound and this specific uptake was readily detected by non-invasive planar imaging [97]. CGS 27023A together with alternative hydroxamate-derivatives were recently labeled with ^{18}F for PET imaging [98, 99]. Preliminary biodistribution studies indicated that there was no tissue-specific accumulation of [^{18}F]-CGS 27023A 1f and [^{18}F]-CGS 27023A 1e in wild-type mice. The preparation of non-hydroxamate derivatives MMPIs has also been described recently [100]. It is expected that on-going studies will quickly determine whether these new agents have potential for the molecular imaging of MMP expression in atherosclerotic plaques.

Apoptosis Imaging

Annexin A5

Kolodgie et al. [101] first demonstrated the feasibility of non-invasive imaging of apoptosis using [^{99m}Tc]-Annexin A5 in experimental atherosclerotic lesion induced by deendothelialization of the infradiaphragmatic aorta in rabbits fed a high-cholesterol diet. The rapid blood kinetics of the tracer allowed in vivo planar imaging to be performed 2 hours following injection, and a positive correlation was observed between [^{99m}Tc]-Annexin A5 uptake and macrophage burden or apoptosis but not with SMC. The feasibility of in vivo planar imaging of apoptosis with [^{99m}Tc]-Annexin A5 was confirmed in an experimental model of genetically hypercholesterolemic rabbits [63]. Johnson et al. [102] provided in vivo SPECT images of [^{99m}Tc]-Annexin A5 uptake in injured coronary arteries of swines also fed a high-cholesterol diet, a model characterized by predominant smooth muscle cell apoptosis. Thirteen out of 22 injured vessels showed focal tracer uptake, and scan-positive vessels had a significantly higher apoptotic index than scan-negative vessels. Dedicated small animal imaging equipment recently allowed tomographic imaging of aortic atherosclerotic lesions in mouse models of plaque development [103] as demonstrated in Fig. (**5**). Several experimental studies indicated that variations in the apoptotic status of experimental atherosclerotic lesions could be monitored with [^{99m}Tc]-Annexin A5. Hartung et al. [104] showed that dietary modification and statin therapy decreased [^{99m}Tc]-Annexin A5 uptake by ex vivo imaging and γ-well counting in a rabbit model of atherosclerosis induced by deendothelialization of the abdominal aorta. The inhibitory effect of broad and specific caspase inhibition on apoptosis as assessed with [^{99m}Tc]-Annexin A5 in vivo SPECT imaging was also recently studied on a similar experimental model [105]. [^{99m}Tc]-Annexin A5 and [^{18}F]-FDG were recently compared in an autoradiographic study for the detection of aortic atherosclerosis in ApoE$^{-/-}$ mice fed a hypercholesterolemic diet. Although the absolute uptake levels of [^{18}F]-FDG in

atherosclerotic lesions were 5- to 6-fold higher, the uptake ratios of advanced-to-early lesions were significantly higher with [^{99m}Tc]-Annexin A5 than with [^{18}F]-FDG. Therefore, [^{99m}Tc]-Annexin A5 might possibly have a greater potential than [^{18}F]-FDG as an indicator of late stage, vulnerable plaques as compared with early lesions [106]. Phase I clinical studies indicated that the biodistribution and dosimetry of [^{99m}Tc]-Annexin A5 were suitable for apoptosis imaging in the abdominal and thoracic area of patients [107]. In a pilot clinical study, Kietselaer et al. [108] evaluated [^{99m}Tc]-Annexin A5 carotid uptake in patients. The results indicated that tracer uptake was visible in those patients with a recent, but not remote, history of transient ischemic attack, and that [^{99m}Tc]-Annexin A5 accumulation correlated with histopathological features of unstable plaques at endarterectomy.

Additional Apoptosis Imaging Agents

Although [^{99m}Tc]-Annexin A5 remains the most largely studied tracer of apoptosis, alternative peptidic and non-peptidic agents have been described [109-113]. The behavior of these new compounds warrant further investigation.

Additional Molecular Targets for Vulnerable Atherosclerosis Imaging

Endothelin Receptors

Since endothelins have been implicated in the pathogenesis of atherosclerosis, endothelin derivatives seemed promising agents for atherosclerosis imaging through binding to endothelin receptors [114, 115]. However, further characterization of 2 rabbit models of atherosclerosis demonstrated that neither the density of overall endothelin receptors nor the density of either endothelin receptor subtype was significantly increased in atherosclerotic aortas. Therefore, the authors concluded that endothelin receptor was not a suitable target for

atherosclerosis imaging [116]. Therefore, the authors concluded that endothelin receptor was not a suitable target for atherosclerosis imaging [116].

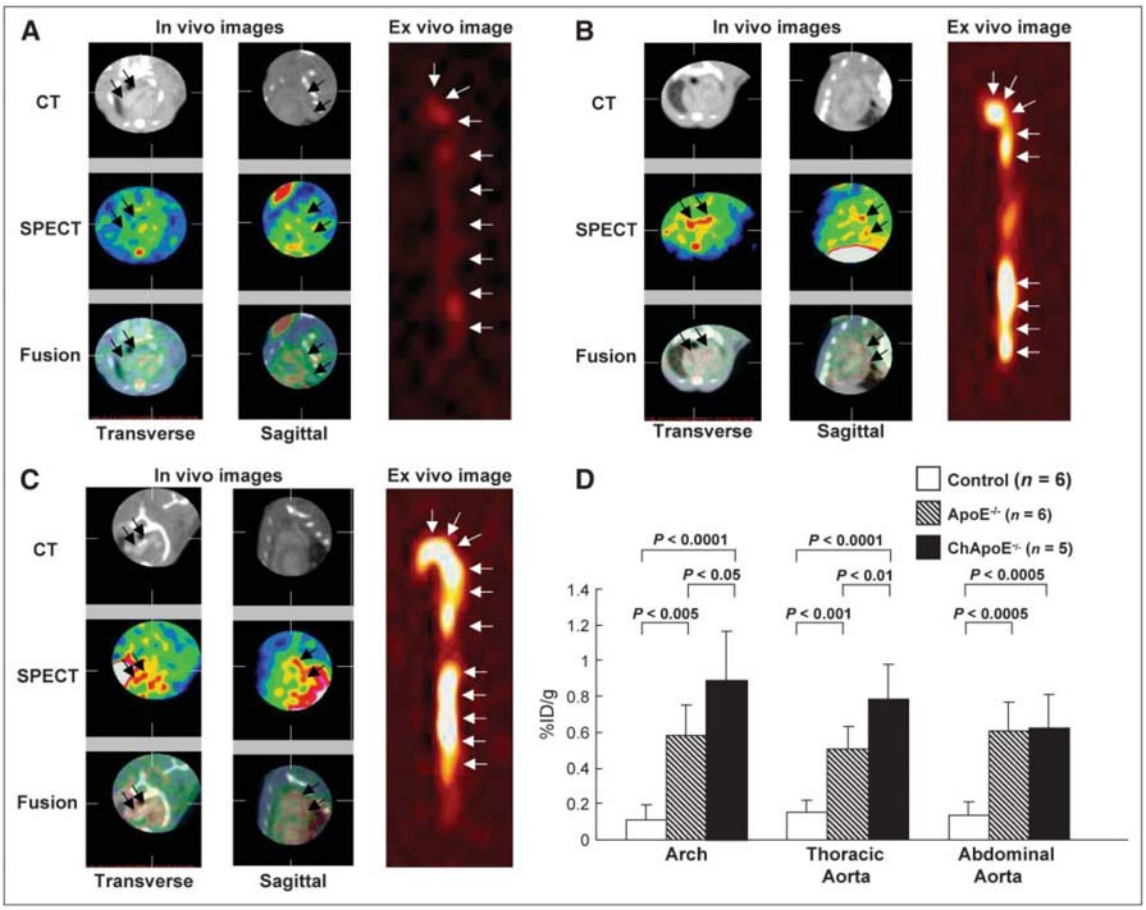

Fig (**5**).Non-invasive in vivo SPECT imaging of apoptosis using [^{99m}Tc]-annexin A5. In vivo and ex vivo images of control mice (A) and apoE$^{-/-}$ mice without cholesterol diet (B) and with cholesterol diet (C). For all images, left panel represents transverse images, middle panel represents sagittal images, and right panel represents ex vivo images (A–C). Top panel shows micro-CT, middle panel shows micro-SPECT, and bottom panel shows fusion images. (A) No obvious [^{99m}Tc]-annexin A5 uptake was seen on either in vivo or ex vivo images of control animals. (B) Distinct uptake was observed in the arch on in vivo images and in the arch and abdominal aorta on ex vivo image. (C) Distinct uptake and calcification were observed in the arch on the in vivo images; [^{99m}Tc]-annexin A5 uptake was seen in whole aorta on the ex vivo image. (D) Quantitative uptake was highest in cholesterol-fed apoE$^{-/-}$ mice, followed by chow-fed apoE$^{-/-}$ and control mice in lesions at arch, thoracic, or abdominal level. Ch = cholesterol fed. Reproduced from [103] with permission the Society of Nuclear Medicine.

Angiogenesis

As described above, angiogenesis has been recently recognized as a major contributor to vulnerable plaque development [39]. An autoradiographic study indicated that the αvβ3

integrin – specific tracer [^{111}In]-RP748 preferentially localized to the atherosclerotic lesion in a hypercholesterolemic mouse model of left carotid artery injury [117].

The extra-domain B (ED-B) is inserted into the fibronectin molecule during angiogenesis. Matter et al. [118] used the human antibody L19 specific against ED-B to perform autoradiographic imaging of plaque neoangiogenesis in aortas of hypercholesterolemic mice. The authors also compared the behaviour of [^{125}I]-L19 with that of [^{125}I]-G11, a radiolabeled antibody specific against the C domain of tenascin-C, which is overexpressed in atherosclerotic plaques and absent from normal adult tissues [119]. Both of these agents seemed to have potential for imaging atherosclerosis providing that enough time is allowed for blood clearance, but no in vivo imaging study is yet available.

Antisense Oligonucleotide Strategy

Finally, recent studies have suggested that different signaling pathways and various cell transcription factors are activated during the early stage of the atherosclerotic process, including proto-oncogenes such as c-fos and c-myc [120, 121]. The activation of proto-oncogenes over the course of atherosclerosis may result in an increase in corresponding mRNA levels, which might represent a suitable target for imaging using radiolabelled antisense oligonucleotides (ASONs). [^{99m}Tc]-labeled ASONs directed against the proto-oncogene c-myc were therefore injected to New Zealand White rabbits fed an high-cholesterol diet. The accumulation of the tracer in the vascular wall correlated with areas of plaque development and could be detected by in vivo planar imaging [122]. However, the ASON strategy remains challenging because of the complexity of in vivo probe delivery. This can mainly be attributed to the low amout of target and to the numerous biological barriers to overcome while maintaining the stability of the probe [123]

CONCLUSION

Over the last decade several radiotracers have been evaluated for the in vivo molecular imaging of vulnerable atherosclerotic plaques. Radiotracers targeted at the inflammatory process seem particularly relevant and promising. [^{99m}Tc]-MCP-1 [64, 65] for SPECT imaging as well as [^{18}F]-FDG [62] for PET imaging both demonstrated the feasibility of in vivo imaging of macrophage recruitment and metabolism within atherosclerotic lesions. In addition, a few tracers have been evaluated clinically. Both [^{99m}Tc]-Annexin A5 [108] for SPECT imaging and [^{18}F]-FDG [66, 67] for PET imaging successfully identified vulnerable atherosclerotic plaques in the carotid vessels of patients. However, nuclear imaging of vulnerable plaques at the level of coronary arteries remains a challenging issue because of the small size of the atherosclerotic lesions, of their vicinity with blood and the unbound, circulating tracer activity, and of the motion of the heart. ECG-gated SPECT or PET acquisitions might be employed to partially overcome the limitation associated with cardiac motion. In the future, in addition to the development of new radiotracers with improved pharmacokinetics, new SPECT and PET multi-modality cameras with better resolution and sensitivity [124] might play a major role in vulnerable plaque imaging using radiolabeled tracers.

REFERENCES

1. AHA. Heart disease and stroke statistics - 2006 update. A report from the American Heart Association statistics committee and stroke statistics subcommittee. *Circulation.,* **2008**, *117*, e25-e146.

2. Fuster, V.; Moreno, P.R.; Fayad, Z.A.; Corti, R.; Badimon, J.J. Atherothrombosis and high-risk plaque: part I: evolving concepts. *J. Am. Coll. Cardiol*., **2005**, *46*, 937-54.

3. Naghavi, M.; Libby, P.; Falk, E.; Casscells, S.W.; Litovsky, S.; Rumberger, J.; Badimon, J.J.; Stefanadis, C.; Moreno, P.; Pasterkamp, G.; Fayad, Z.; Stone, P.H.; Waxman, S.; Raggi, P.; Madjid, M.; Zarrabi, A.; Burke, A.; Yuan, C.; Fitzgerald, P.J.; Siscovick, D.S.; de Korte, C.L.; Aikawa, M.; Juhani Airaksinen, K.E.; Assmann, G.; Becker, C.R.; Chesebro, J.H.; Farb, A.; Galis, Z.S.; Jackson, C.; Jang, I.K.; Koenig, W.; Lodder, R.A.; March, K.; Demirovic, J.; Navab, M.; Priori, S.G.; Rekhter, M.D.; Bahr, R.; Grundy, S.M.; Mehran, R.; Colombo, A.; Boerwinkle, E.; Ballantyne, C.; Insull, W. Jr.; Schwartz, R.S.; Vogel, R.; Serruys, P.W.; Hansson, G.K.; Faxon, D.P.; Kaul, S.; Drexler, H.; Greenland, P.; Muller, J.E.; Virmani, R.; Ridker, P.M.; Zipes, D.P.; Shah, P.K.; Willerson, J.T. From vulnerable plaque to vulnerable patient: a call for new definitions and risk assessment strategies: Part I. *Circulation*., **2003**(a), *108*, 1664-72.

4. Ross, R. Atherosclerosis--an inflammatory disease. *N. Engl. J. Med*., **1999**, *340*, 115-26.

5. Fuster, V.; Fayad, Z.A.; Badimon, J.J. Acute coronary syndromes: biology. *Lancet*., **1999**, *353 Suppl 2*, SII5-9.

6. Malek, A.M.; Alper, S.L.; Izumo S. Hemodynamic shear stress and its role in atherosclerosis. *JAMA*., **1999**, *282*, 2035-42.

7. Glagov, S.; Weisenberg, E.; Zarins, C.K.; Stankunavicius, R.; Kolettis, G.J. Compensatory enlargement of human atherosclerotic coronary arteries. *N. Engl. J. Med*., **1987**, *316*, 1371-5.

8. De Franco, A.C.; Nissen, S.E. Coronary intravascular ultrasound: implications for understanding the development and potential regression of atherosclerosis. *Am. J. Cardiol*., **2001**, *88*, 7M-20M.

9. Naghavi, M.; Libby, P.; Falk, E.; Casscells, S.W.; Litovsky, S.; Rumberger, J.; Badimon, J.J.; Stefanadis, C.; Moreno, P.; Pasterkamp, G.; Fayad, Z.; Stone, P.H.; Waxman, S.; Raggi, P.; Madjid, M.; Zarrabi, A.; Burke, A.; Yuan, C.; Fitzgerald, P.J.; Siscovick, D.S.; de Korte, C.L.; Aikawa, M.; Airaksinen K.E.; Assmann, G.; Becker, C.R.; Chesebro, J.H.; Farb, A.;

Galis, Z.S.; Jackson, C.; Jang, I.K.; Koenig, W.; Lodder, R.A.; March, K.; Demirovic, J.; Navab, M.; Priori, S.G.; Rekhter, M.D.; Bahr, R.; Grundy, S.M.; Mehran, R.; Colombo, A.; Boerwinkle, E.; Ballantyne, C.; Insull, W. Jr.; Schwartz, R.S.; Vogel, R.; Serruys, P.W.; Hansson, G.K.; Faxon, D.P.; Kaul, S.; Drexler, H.; Greenland, P.; Muller, J.E.; Virmani, R.; Ridker, P.M.; Zipes, D.P.; Shah, P.K.; Willerson, J.T. From vulnerable plaque to vulnerable patient: a call for new definitions and risk assessment strategies: Part II. *Circulation*., **2003**(b), *108*, 1772-8.

10. Schaar J.A.; Mastik F.; Regar E.; den Uil C.A.; Gijsen F.J.; Wentzel J.J.; Serruys P.W.; van der Stehen A.F. Current diagnostic modalities for vulnerable plaque detection. *Curr. Pharm; Des.* **2007**;13:995-1001.

11. Naghavi, M.; Falk, E.; Hecht, H.S.; et al. From vulnerable plaque to vulnerable patient: Part III: Executive summary of the Screening for Heart Attack Prevention and Education (SHAPE) Task Force report. *Am. J. Cardiol*., **2006**, *98*, 2H-15H.

12. Davies, J.R.; Rudd, J.H.; Weissberg, P.L.; Narula, J. Radionuclide imaging for the detection of inflammation in vulnerable plaques. *J. Am. Coll. Cardiol*., **2006**, *47*, C57-68.

13. Del Guerra, A.; Belcari, N. State-of-the-art of SPECT, PET, and CT for small animal imaging. *Nuclear Instruments and Methods in Physics Research A.*, **2007**, *583*, 119–124.

14. Franc, B.L.; Acton, P.D.; Mari, C.; Hasegawa, B.H. Small animal SPECT and SPECT/CT: important tools for preclinical investigation. *J; Nucl. Med*., **2008**, *49*, 1651-63.

15. Stary, H.C.; Chandler, A.B.; Glagov, S.; Guyton, J.R.; Insull, W. Jr.; Rosenfeld, M.E.; Schaffer, S.A.; Schwartz, C.J.; Wagner, W.D.; Wissler, R.W. A definition of initial, fatty streak, and intermediate lesions of atherosclerosis. A report from the Committee on Vascular Lesions of the Council on Arteriosclerosis, American Heart Association. *Circulation*., **1994**, *89*, 2462-78.

16. Stary, H.C.; Chandler, A.B.; Dinsmore, R.E.; Fuster, V.; Glagov, S.; Insul,l W. Jr.; Rosenfeld, M.E.; Schwartz, C.J.; Wagner, W.D.; Wissler, R.W. A definition of advanced types of atherosclerotic lesions and a histological classification of atherosclerosis. A report from the Committee on Vascular Lesions of the Council on Arteriosclerosis, American Heart Association. *Circulation.*, **1995**, *92*, 1355-74.

17. Stary, H. *Atlas of atherosclerosis - progression and regression*. Parthenon Publishing: New York, **1999**.

18. Virmani, R.; Kolodgie, F.D.; Burke, A.P.; Farb, A.; Schwartz, S.M. Lessons from sudden coronary death: a comprehensive morphological classification scheme for atherosclerotic lesions. *Arterioscler. Thromb. Vasc. Biol.*, **2000**, *20*, 1262-75.

19. Chatzizisis, Y.S.; Coskun, A.U.; Jonas, M.; Edelman, E.R.; Feldman, C.L.; Stone, P.H. Role of endothelial shear stress in the natural history of coronary atherosclerosis and vascular remodeling: molecular, cellular, and vascular behavior. *J. Am. Coll. Cardiol.*, **2007**, *49*, 2379-93.

20. Harrison, D.G.; Widder, J.; Grumbach, I.; Chen, W.; Weber, M.; Searles, C. Endothelial mechanotransduction, nitric oxide and vascular inflammation. *J. Intern. Med.*, **2006**, *259*, 351-63.

21. Collins, T.; Cybulsky, M.I. NF-kappaB: pivotal mediator or innocent bystander in atherogenesis? *J. Clin. Invest.*, **2001**, *107*, 255-64.

22. Kinlay, S.; Libby, P.; Ganz, P. Endothelial function and coronary artery disease. *Curr. Opin. Lipidol.*, **2001**, *12*, 383-9.

23. Ley, K.; Huo, Y. VCAM-1 is critical in atherosclerosis. *J. Clin. Invest.*, **2001**, *107*, 1209-10.

24. Steinberg, D. Atherogenesis in perspective: hypercholesterolemia and inflammation as partners in crime. *Nat. Med.*, **2002**, *8*, 1211-7.

25. Chitu, V.; Stanley, ER. Colony-stimulating factor-1 in immunity and inflammation. *Curr. Opin. Immunol*., **2006**, *18*, 39-48.

26. Dunn, S.; Vohra, R.S.; Murphy, J.E.; Homer-Vanniasinkam, S.; Walker, J.H.; Ponnambalam, S. The lectin-like oxidized low-density-lipoprotein receptor: a pro-inflammatory factor in vascular disease. *Biochem. J*., **2008**, *409*, 349-55.

27. Pasterkamp, G.; Van Keulen, J.K.; De Kleijn, D.P. Role of Toll-like receptor 4 in the initiation and progression of atherosclerotic disease. *Eur. J. Clin. Invest*., **2004**, *34*, 328-34.

28. Schoneveld, A.H.; Hoefer, I.; Sluijter, J.P.; Laman, J.D.; de Kleijn, D.P.; Pasterkamp, G. Atherosclerotic lesion development and Toll like receptor 2 and 4 responsiveness. *Atherosclerosis*., **2008**, *197*, 95-104.

29. Glass, C.K.; Witztum, J.L. Atherosclerosis. the road ahead. *Cell*., **2001**, *104*, 503-16.

30. Mach, F.; Schönbeck, U.; Bonnefoy, J.Y.; Pober, J.S.; Libby, P. Activation of monocyte/macrophage functions related to acute atheroma complication by ligation of CD40: induction of collagenase, stromelysin, and tissue factor. *Circulation*., **1997**, *96*, 396-9.

31. Lutgens, E.; Lievens, D.; Beckers, L.; Donners, M.; Daemen, M. CD40 and its ligand in atherosclerosis. *Trends Cardiovasc. Med*., **2007**, *17*, 118-23.

32. Galis, Z.S. Vulnerable plaque: the devil is in the details. *Circulation*., **2004**, *110*, 244-6.

33. Newby, A.C. Do metalloproteinases destabilize vulnerable atherosclerotic plaques? *Curr. Opin. Lipidol*., **2006**, *17*, 556-61.

34. Steffel, J.; Lüscher, T.F.; Tanner, F.C. Tissue factor in cardiovascular diseases: molecular mechanisms and clinical implications. *Circulation*., **2006**, *113*, 722-31.

35. Tedgui, A.; Mallat, Z. Apoptosis as a determinant of atherothrombosis. *Thromb. Haemost*., **2001**, *86*, 420-6.

36. Newby, A.C.; Zaltsman, A.B. Fibrous cap formation or destruction-the critical importance of vascular smooth muscle cell proliferation, migration and matrix formation. *Cardiovasc. Res.*, **1999**, *41*, 345-60.

37. Doran, A.C.; Meller, N.; McNamara, C.A. Role of smooth muscle cells in the initiation and early progression of atherosclerosis. *Arterioscler. Thromb. Vasc. Biol.*, **2008**, *28*, 812-9.

38. O'Brien, K.D.; McDonald, T.O.; Chait, A.; Allen, M.D.; Alpers, C.E. Neovascular expression of E-selectin, intercellular adhesion molecule-1, and vascular cell adhesion molecule-1 in human atherosclerosis and their relation to intimal leukocyte content. *Circulation.*, **1996**, *93*, 672-82.

39. Moreno, P.R.; Purushothaman, K.R.; Fuster, V.; Echeverri, D.; Truszczynska, H.; Sharma, SK.; Badimon, J.J.; O'Connor, W.N. Plaque neovascularization is increased in ruptured atherosclerotic lesions of human aorta: implications for plaque vulnerability. *Circulation.*, **2004**, *110*, 2032-8.

40. Doyle, B.; Caplice, N. Plaque neovascularization and antiangiogenic therapy for atherosclerosis. *J. Am. Coll. Cardiol.*, **2007**, *49*, 2073-80.

41. Burke, A.P.; Farb, A.; Malcom, GT.; Liang, Y.H.; Smialek, J.; Virmani, R. Coronary risk factors and plaque morphology in men with coronary disease who died suddenly. *N Engl J Med.*, **1997**, *336*, 1276-82.

42. Lees, R.S.; Lees, A.M.; Strauss, H.W. External imaging of human atherosclerosis. *J. Nucl. Med.*, **1983,** *24*, 154-156.

43. Lees, R.S.; Garabedian, H;D.; Lees, A.M.; Schumacher, D.J.; Miller, A.; Isaacsohn, J.L.; Derksen, A.; Strauss, H.W. Technetium-99m low density lipoproteins: preparation and biodistribution. *J. Nucl. Med.*, **1985,** *26*, 1056-62.

44. Vallabhajosula, S.; Paidi, M.; Badimon, J.J.; Le, N.A.; Goldsmith, S.J.; Fuster, V.; Ginsberg, H.N. Radiotracers for low density lipoprotein biodistribution studies in vivo:

technetium-99m low density lipoprotein versus radioiodinated low density lipoprotein preparations. *J. Nucl. Med*., **1988**, *29,* 1237-45.

45. Lees, A.M.; Lees, R.S.; Schoen, F.J.; Isaacsohn, J.L.; Fischman, A.J.; McKusick, K.A.; Strauss, H.W. Imaging human atherosclerosis with 99mTc-labeled low density lipoproteins. *Arteriosclerosis*., **1988,** *8*, 461-470.

46. Rosen, J.M.; Butler, S.P.; Meinken, G.E.; Wang, T.S.; Ramakrishnan, R.; Sristava, S.C.; Alderson, P.O.; Ginsberg, H.N. Indium-111-labeled LDL: a potential agent for imaging atherosclerotic disease and lipoprotein biodistribution. *J. Nucl. Med*., **1990**, *31,* 343-350.

47. Hay, R.V.; Fleming, R;M.; Ryan, J.W.; Williams, K.A.; Stark, V.J.; Lathrop, K.A.; Harper, PV. Nuclear imaging analysis of human low-density lipoprotein biodistribution in rabbits and monkeys. *J. Nucl. Med*., **1991**, *32*, 1239-1245.

48. Virgolini, I.; Angelberger, P.; O'Grady, J.; Sinzinger, H. Low density lipoprotein labelling characterizes experimentally induced atherosclerotic lesions in rabbits in vivo as to presence of foam cells and endothelial coverage. *Eur. J. Nucl. Med*., **1991**, *18*, 944-947.

49. Pirich, C.; Sinzinger, H. Evidence for lipid regression in humans in vivo performed by 123Iodine-low-density lipoprotein scintiscanning. *Ann. N Y Acad. Sci*., **1995,** *748*, 613-21.

50. Iuliano, L.; Signore, A.; Vallabajosula, S.; Colavita, A.R.; Camastra, C.; Ronga, G.; Alessandri, C.; Sbarigia, E.; Fiorani, P.; Violi, F. Preparation and biodistribution of 99m technetium labelled oxidized LDL in man. *Atherosclerosis*., **1996,** *126*, 131-41.

51. Hardoff, R.; Braegelmann, F.; Zanzonico, P.; Herrold, E.M.; Lees, R.S.; Lees, A.M.; Dean, R.T.; Lister-James, J.; Borer, J.S. External imaging of atherosclerosis in rabbits using an 123I-labeled synthetic peptide fragment. *J. Clin. Pharmacol*., **1993,** *33*, 1039-47.

52. Hardoff, R.; Zanzonico, P.; Braegelmann, F.; Herrold, E.M.; Lees, R.S.; Lees, A.M.; Dean, R;T.; Lister-James, J.; Borer, J.S. Localization of (99m)Tc-labeled apoB synthetic

peptide in arterial lesions of an experimental model of spontaneous atherosclerosis. *Am. J. Ther*., **1995,** *2*, 88-99.

53. Tsimikas, S.; Palinski, W.; Halpern, S.E.; Yeung, D.W.; Curtiss, L.K.; Witztum, J.L. Radiolabeled MDA2, an oxidation-specific, monoclonal antibody, identifies native atherosclerotic lesions in vivo. *J. Nucl. Cardiol*., **1999,** *6*, 41-53.

54. Torzewski, M.; Shaw, P.X.; Han, K.R.; Shortal, B.; Lackner, K.J.; Witztum, J.L.; Palinski, W.; Tsimikas, S. Reduced in vivo aortic uptake of radiolabeled oxidation-specific antibodies reflects changes in plaque composition consistent with plaque stabilization. *Arterioscler. Thromb. Vasc. Biol*., **2004,** *24*, 2307-12.

55. Tsimikas, S.; Shortal, B.P.; Witztum, J.L.; Palinski, W. In vivo uptake of radiolabeled MDA2.; an oxidation-specific monoclonal antibody.; provides an accurate measure of atherosclerotic lesions rich in oxidized LDL and is highly sensitive to their regression. *Arterioscler. Thromb. Vasc. Biol*., **2000**, *20,* 689-97.

56. Shaw, P.X.; Hörkkö, S.; Tsimikas, S.; Chang, M.K.; Palinski, W.; Silverman, G.J.; Chen, P.P.; Witztum, J.L. Human-derived anti-oxidized LDL autoantibody blocks uptake of oxidized LDL by macrophages and localizes to atherosclerotic lesions in vivo. *Arterioscler. Thromb. Vasc. Biol*., **2001,** *21*, 1333-9.

57. Tsimikas, S.Noninvasive imaging of oxidized low-density lipoprotein in atherosclerotic plaques with tagged oxidation-specific antibodies. *Am. J. Cardiol*., **2002,** *90*, 22L-27L.

58. Langer, H.F.; Haubner, R.; Pichler, B.J.; Gawaz, M. Radionuclide imaging: a molecular key to the atherosclerotic plaque. *J. Am. Coll. Cardiol*., **2008,** *52*, 1-12.

59. Vohra, R.S.; Murphy, J.E.; Walker, J.H.; Ponnambalam, S.; Homer-Vanniasinkam, S. Atherosclerosis and the Lectin-like OXidized low-density lipoprotein scavenger receptor. *Trends Cardiovasc. Med*., **2006**, *16,* 60-4.

60. Kataoka, H.; Kume, N.; Miyamoto, S.; Minami, M.; Moriwaki, H.; Murase, T.; Sawamura, T.; Masaki, T.; Hashimoto, N.; Kita, T. Expression of lectinlike oxidized low-density lipoprotein receptor-1 in human atherosclerotic lesions. *Circulation*., **1999,** *99*, 3110-7.

61. Ishino, S.; Mukai, T.; Kuge, Y.; Kume, N.; Ogawa, M.; Takai, N.; Kamihashi, J.; Shiomi, M.; Minami, M.; Kita, T.; Saji, H. Targeting of lectinlike oxidized low-density lipoprotein receptor 1 (LOX-1) with 99mTc-labeled anti-LOX-1 antibody: potential agent for imaging of vulnerable plaque. *J. Nucl. Med*., **2008**, *49*, 1677-85.

62. Ogawa, M.; Ishino, S.; Mukai, T.; Asano, D.; Teramoto, N.; Watabe, H.; Kudomi, N.; Shiomi, M.; Magata, Y.; Iida, H.; Saji, H. (18)F-FDG accumulation in atherosclerotic plaques: immunohistochemical and PET imaging study. *J. Nucl. Med*., **2004,** *45*, 1245–50.

63. Ishino, S.; Kuge, Y.; Takai, N.; Tamaki, N.; Strauss, H.W.; Blankenberg, F.G.; Shiomi, M.; Saji, H. 99mTc-Annexin A5 for noninvasive characterization of atherosclerotic lesions: imaging and histological studies in myocardial infarction-prone Watanabe heritable hyperlipidemic rabbits. *Eur. J. Nucl. Med. Mol. Imaging*., **2007,** *34*, 889-99.

64. Ohtsuki, K.; Hayase, M.; Akashi, K.; Kopiwoda, S.; Strauss H.W. Detection of monocyte chemoattractant protein-1 receptor expression in experimental atherosclerotic lesions: an autoradiographic study. *Circulation*., **2001**, *104,* 203-8.

65. Hartung, D.; Petrov, A.; Haider, N.; Fujimoto, S.; Blankenberg, F.; Fujimoto, A.; Virmani, R.; Kolodgie, F.D.; Strauss, HW.; Narula, J. Radiolabeled Monocyte Chemotactic Protein 1 for the detection of inflammation in experimental atherosclerosis. *J. Nucl. Med*., **2007**, *48*, 1816-21.

66. Rudd, J.H.; Warburton, E.A.; Fryer, T.D.; Jones, H.A.; Clark, J.C.; Antoun, N.; Johnström, P.; Davenport, A.P.; Kirkpatrick, P.J.; Arch, B.N.; Pickard, J.D.; Weissberg P.L.

Imaging atherosclerotic plaque inflammation with [18F]-fluorodeoxyglucose positron emission tomography. *Circulation.*, **2002**, *105*, 2708–11.

67. Rudd, J.H.; Myers, K.S.; Bansilal, S.; Machac, J.; Rafique, A.; Farkouh, M.; Fuster, V.; Fayad, ZA. (18)Fluorodeoxyglucose positron emission tomography imaging of atherosclerotic plaque inflammation is highly reproducible: implications for atherosclerosis therapy trials. *J. Am. Coll. Cardiol.*, **2007,** *50*, 892-6.

68. Tawakol, A.; Migrino, R.Q.; Hoffmann, U.; Abbara, S.; Houser, S.; Gewirtz, H.; Muller, J.E.; Brady, T.J.; Fischman, A.J. Noninvasive in vivo measurement of vascular inflammation with F-18 fluorodeoxyglucose positron emission tomography. *J. Nucl. Cardiol*., **2005,** *12*, 294-301.

69. Tawakol, A.; Migrino, R.Q.; Bashian, G.G.; Bedri, S.; Vermylen, D.; Cury, R.C.; Yates, D.; LaMuraglia, G.M.; Furie, K.; Houser, S.; Gewirtz, H.; Muller, J.E.; Brady, T.J.; Fischman, A.J. In vivo 18Ffluorodeoxyglucose positron emission tomography imaging provides a noninvasive measure of carotid plaque inflammation in patients. *J. Am. Coll. Cardiol.*, **2006**, *48*, 1818 –24.

70. Calcagno, C.; Cornily, J.C.; Hyafil, F.; Rudd, J.H.; Briley-Saebo, K.C.; Mani, V.; Goldschlager, G.; Machac, J.; Fuster, V.; Fayad, Z. Detection of neovessels in atherosclerotic plaques of rabbits using dynamic contrast enhanced MRI and 18F-FDG PET. *Arterioscler. Thromb. Vasc. Biol*., **2008,** *28*, 1311-7.

71. Tahara, H.; Kai, H.; Nakaura, H.; Mizoguchi, M.; Ishibashi, M.; Kaida, H.; Baba, K.; Hayabuchi, N.; Imaizumi, T. The prevalence of inflammation in carotid atherosclerosis: analysis with fluorodeoxyglucose-positron emission tomography. *Eur. Heart. J*., **2007**(a), *28*, 2243-48.

72. Tahara, H.; Kai, H.; Yamagishi ,S.; Mizoguchi, M.; Nakaura, H.; Ishibashi, M.; Kaida, H.; Baba, K.; Hayabuchi, N.; Imaizumi, T. Vascular inflammation evaluated by [18F]-

fluorodeoxyglucose positron emission tomography is associated with the metabolic syndrome. *J. Am. Coll. Cardiol*., **2007**(b), *49*, 1533-9.

73. Tahara, N.; Kai, H.; Ishibashi, M.; Nakaura, H.; Kaida, H.; Baba, K.; Hayabuchi, N.; Imaizumi T. Simvastatin attenuates plaque inflammation: evaluation by fluorodeoxyglucose positron emission tomography. *J. Am. Coll. Cardiol.*, **2006**, *48*, 1825–31.

74. Ogawa, M.; Magata, Y.; Kato, T.; Hatano, K.; Ishino, S.; Mukai, T.; Shiomi, M.; Ito, K.; Saji, H. Application of 18F-FDG-PET for monitoring the therapeutic effect of antiinflammatory drugs on stabilization of vulnerable atherosclerotic plaques. *J. Nucl. Med.*, **2006,** *47*, 1845–50.

75. Laurberg, J.M.; Olsen, A.K.; Hansen, S.B.; Bottcher, M.; Morrison, M.; Ricketts, S.A.; Falk, E. Imaging of vulnerable atherosclerotic plaques with FDG-microPET: no FDG accumulation. *Atherosclerosis*., **2007**, *192*, 275-82.

76. Rudd, J.H.; Fayad, Z.A.; Machac, J.; Weissberg, P.L.; Davies, J.R.; Warburton, E.A.; Tawakol, A.A.; Strauss, H.W.; Fuster, V. Response to 'Laurberg, J.M.; Olsen, A.K.; Hansen, S.B.; et al. Imaging of vulnerable atherosclerotic plaques with FDG-microPET: no FDG accumulation' [*Atherosclerosis* 2006]. *Atherosclerosis.*, **2007**, *192*, 453-4; author reply 451-2.

77. Lederman, R.J.; Raylman, R.R.; Fisher, S.J.; Kison, P.V.; San, H.; Nabel, E.G.; Wahl, R.L. Detection of atherosclerosis using a novel positron-sensitive probe and 18-fluorodeoxyglucose (FDG). *Nucl Med Commun*., **2001**, *22*, 747-53.

78. Mukai, T.; Nohara, R.; Ogawa, M.; Ishino, S.; Kambara, N.; Kataoka, N.; Kanoi, T.; Saito, K.; Motomura, H.; Konishi, J.; Saji, H. A catheter-based radiation detector for endovascular detection of atheromatous plaques. *Eur. J. Nucl. Med. Mol. Imaging*., **2004**, *31*, 1299-303.

79. Hosokawa, R.; Kambara, N.; Ohba, M.; Mukai, T.; Ogawa, M.; Motomura, H.; Kume, N.; Saji, H.; Kita, T.; Nohara, R. A catheter-based intravascular radiation detector of vulnerable plaques. *J. Nucl. Med*., **2006,** *47*, 863-7.

80. Strauss, H.W.; Mari, C.; Patt, B.E.; Ghazarossian, V. Intravascular radiation detectors for the detection of vulnerable atheroma. *J. Am. Coll. Cardiol*., **2006**, *47*, C97-C100.

81. Shikhaliev, P.M.; Xu, T.; Ducote, J.L.; Easwaramoorthy, B.; Mukherjee, J.; Molloi, S. Positron autoradiography for intravascular imaging: feasbility evaluation. *Phys. Med. Biol*., **2006**, *51*, 963-79.

82. Schmid, D.T.; John, H.; Zweifel, R.; Cservenyak, T.; Westera, G.; Goerres, G.W.; von Schulthess, G.K.; Hany, T.F. Fluorocholine PET/CT in patients with prostate cancer: initial experience. *Radiology*., **2005,** *235*, 623-8.

83. Boggs, K.P.; Rock, C.O.; Jackowski, S. Lysophosphatidylcholine and 1-Ooctadecyl-2-O-methyl-rac-glycero-3-phosphocholine inhibit the CDPcholine pathway of phosphatidylcholine synthesis at the CTP: phosphocholine cytidylyltransferase step. *J. Biol. Chem.*, **1995,** *270*, 7757–64.

84. Wyss, M.T.; Weber, B.; Hoenr, M.; Späth, N.; Ametamey, S.M.; Westera, G.; Bode, B.; Kaim, A.H.; Buck, A. 18F-choline in experimental soft tissue infection assessed with autoradiography and high-resolution PET. *Eur. J. Nucl. Med. Mol. Imaging*., **2004,** *31*, 312-6.

85. Spaeth, N.; Wyss, M.T.; Weber, B.; Scheidegger, S.; Lutz, A.; Verwey, J.; Radovanovic, I.; Pahnke, J.; Wild, D.; Westera, G.; Weishaupt, D.; Hermann, D.M.; Kaser-Hotz, B.; Aguzzi A.; Buck A. Uptake of 18F-fluorocholine.; 18F-fluoroethyl-L-tyrosine.; and 18F-FDG in acute cerebral radiation injury in the rat: implications for separation of radiation necrosis from tumor recurrence. *J. Nucl. Med*., **2004,** *45*, 1931-8.

86. Matter, C.M.; Wyss, M.T.; Meier, P.; Späth, N.; von Lukowicz, T.; Lohmann, C.; Weber, B.; Ramirez de Molina, A.; Lacal J.C.; Ametamey, S.M.; von Schulthess, G.K.; Lüscher T.F.;

Kaufmann, P.A.; Buck, A. 18F-choline images murine atherosclerotic plaques ex vivo. *Arterioscler. Thromb. Vasc. Biol*., **2006,** *26*, 584-9.

87. Kircher, M.F.; Grimm, J.; Swirski, F.K.; Libby, P.; Gerszten, R.E.; Allport, J.R.; Weissleder R. Noninvasive in vivo imaging of monocyte trafficking to atherosclerotic lesions. *Circulation*., **2008,** *22*, 388-95.

88. Nahrendorf, M.; Zhang, H.; Hembrador, S.; Panizzi, P.; Sosnovik, D.E.; Aikawa, E.; Libby, P.; Swirski, F.K.; Weissleder, R. Nanoparticle PET-CT imaging of macrophages in inflammatory atherosclerosis. *Circulation.*, **2008,** *117*, 379-87.

89. Hamilton, A.J.; Huang, S.L.; Warnick, D.; Rabbat, M.; Kane, B.; Nagaraj, A.; Klegerman, M.; McPherson, D.D. Intravascular ultrasound molecular imaging of atheroma components in vivo. *J. Am. Coll. Cardiol.*, **2004,** *43*, 453-60.

90. Kelly, K.A.; Allport, J.R.; Tsourkas, A.; Shinde-Patil, V.R.; Jospehson, L.; Weissleder R. Detection of vascular adhesion molecule-1 expression using a novel multimodal nanoparticle. *Circ. Res.*, **2005,** *96*, 327-36.

91. Nahrendorf, M.; Jaffer, F.A.; Kelly, K.A.; Sosnovik, D.E.; Aikawa, E.; Libby, P.; Weissleder R. Noninvasive vascular cell adhesion molecule-1 imaging identifies inflammatory activation of cells in atherosclerosis. *Circulation.*, **2006,** *114*, 1504-11.

92. Kaufmann, B.A.; Sanders, J.M.; Davis, C.; Xie, A.; Aldred, P.; Sarembock, I.J.; Lindner, J.R. Molecular imaging of inflammation in atherosclerosis with targeted ultrasound detection of vascular cell adhesion molecule-1. *Circulation*., **2007,** *116*, 276-84.

93. Broisat, A.; Riou, L.M.; Ardisson, V.; Boturyn, D.; Dumy, P.; Fagret, D.; Ghezzi, C. Molecular imaging of vascular cell adhesion molecule-1 expression in experimental atherosclerotic plaques with radiolabelled B2702-p. *Eur. J. Nucl. Med. Mol. Imaging*., **2007,** *34*, 830-40.

94. Ling, X.; Tamaki, T.; Xiao, Y.; Kamangar, S.; Clayberger, C.; Lewis, D.B.; Krensky, A.M. An immunosuppressive and anti-inflammatory HLA class I-derived peptide binds vascular cell adhesion molecule-1. *Transplantation*., **2000,** *27*, 662-7.

95. Dimastromatteo, J.; Ahmadi, M.; Broisat, A.; Riou, L.M.; Boturyn, D.; Dumy, P.; Fagret, D.; Ghezzi, C. In Vivo Molecular Imaging of Vascular Cell Adhesion Molecule-1 Expression in Atherosclerotic Plaques [Oral communication]. Annual Congress of the European Association of Nuclear Medicine, October 11th – 15th, **2008**, Munich, Germany.

96. Kopka, K.; Breyholz, H.J.; Wagner, S.; Law, M.P.; Riemann, B.; Schröer, S.; Trub, M.; Guilbert, B.; Levkau, B.; Schober, O.; Schäfers, M. Synthesis and preliminary biological evaluation of new radioiodinated MMP inhibitors for imaging MMP activity in vivo. *Nucl. Med. Biol*., **2004,** *31*, 257-67.

97. Schäfers, M.; Riemann, B.; Kopka, K.; Breyholz, H.J.; Wagner, S.; Schäfers, K.P.; Law, M.P.; Schober, O.; Levkau, B. Scintigraphic imaging of matrix metalloproteinase activity in the arterial wall in vivo. *Circulation*., **2004,** *109*, 2554-9.

98. Breyholz, H.J.; Wagner, S.; Levkau, B.; Schober, O.; Schäfers, M.; Kopka, K. A 18F-radiolabeled analogue of CGS 27023A as a potential agent for assessment of matrix-metalloproteinase activity in vivo. *Q. J. Nucl. Med. Mol. Imaging*., **2007,** *51*, 24-32.

99. Wagner, S.; Breyholz, H.J.; Law, M.P.; Faust, A.; Höltke, C.; Schröer, S.; Haufe, G.; Levkau, B.; Schober, O.; Schäfers, M.; Kopka, K. Novel fluorinated derivatives of the broad-spectrum MMP inhibitors N-hydroxy-2(R)-[[(4-methoxyphenyl)sulfonyl](benzyl)- and (3-picolyl)-amino]-3-methyl-butanamide as potential tools for the molecular imaging of activated MMPs with PET. *J. Med. Chem*., **2007,** *50*, 5752-5764.

100. Breyholz, H.J.; Schäfers, M.; Wagner, S.; Hôltke, C.; Faust, A.; Rabeneck, H.; Levkau, B.; Schober, O.; Kopka, K. C-5-disubstituted barbiturates as potential molecular probes for noninvasive matrix metalloproteinase imaging. *J. Med. Chem*., **2005,** *48*, 3400-09.

101. Kolodgie, F.D.; Petrov, A.; Virmani, R.; Narula, N.; Verjans, J.W.; Weber, D.K.; Hartung, D.; Steinmetz, N.; Vanderheyden, J.L.; Vannan, M.A.; Gold, H.K.; Reutelingsperger, C.P.; Hofstra, L.; Narula, J. Targeting of apoptotic macrophages and experimental atheroma with radiolabeled annexin V: a technique with potential for noninvasive imaging of vulnerable plaque *Circulation*., **2003,** *108*, 3134-9.

102. Johnson, L.L.; Schofield, L.; Donahay, T.; Narula, N.; Narula J. 99mTc-annexin V imaging for in vivo detection of atherosclerotic lesions in porcine coronary arteries. *J. Nucl. Med*., **2005,** *46*, 1186-93.

103. Isobe, S.; Tsimikas, S.; Zhou, J.; Fujimoto, S.; Sarai, M.; Branks, M.J.; Fujimoto, A.; Hofstra, L.; Reutelingsperger, C.P.; Murohara, T.; Virmani, R.; Kolodgie, F.D.; Narula, N.; Petrov, A.; Narula, J. Noninvasive imaging of atherosclerotic lesions in apolipoprotein E-deficient and low-density-lipoprotein receptor-deficient mice with annexin A5. *J. Nucl. Med*., **2006,** *47*, 1497-505.

104. Hartung, D.; Sarai, M.; Petrov, A.; Kolodgie, F.; Narula, N.; Verjans, J.; Virmani, R.; Reutelingsperger, C.; Hofstra, L.; Narula, J. Resolution of apoptosis in atherosclerotic plaque by dietary modification and statin therapy. *J. Nucl. Med*., **2005,** *46*, 2051-6.

105. Sarai, M.; Hartung, D.; Petrov, A.; Zhou, J.; Narula, N.; Hofstra, L.; Kolodgie, F.; Isobe, S.; Fujimoto, S.; Vanderheyden, J.L.; Virmani, R.; Reutelingsperger, C.; Wong, N.D.; Gupta, S.; Narula, J. Broad and specific caspase inhibitor-induced acute repression of apoptosis in atherosclerotic lesions evaluated by radiolabeled annexin A5 imaging. *J. Am. Coll. Cardiol*., **2007,** *50*, 2305-12.

106. Zhao, Y.; Kuge, Y.; Zhao, S.; Morita, K.; Inubushi, M.; Strauss, H.W.; Blankenberg, F.G.; Tamaki, N. Comparison of 99mTc-annexin A5 with 18F-FDG for the detection of atherosclerosis in ApoE-/- mice. *Eur. J. Nucl. Med. Mol. Imaging*., **2007,** *34*, 1747-1755.

107. Kemerink, G.J.; Liu, X.; Kieffer, D.; Ceyssens, S.; Mortelmans, L.; Verbruggen, A.M.; Steinmetz, N.D.; Vanderheyden, J.L.; Green, A.M.; Verbeke, K. *J. Nucl. Med*., **2003**, *44*, 947-52.

108. Kietselaer, B.L.; Reutelingsperger, C.P.; Heidendal, G.A.; Daemen, M.J.; Mess, W.H.; Hofstra, L.; Narula, J. Noninvasive detection of plaque instability with use of radiolabeled annexin A5 in patients with carotid-artery atherosclerosis. *N. Engl. J. Med*., **2004,** *350*, 1472-3.

109. Elmaleh, D.R.; Narula, J.; Babich, J.W.; Petrov, A.; Fischman, A.J.; Khaw, B.A.; Rapaport, E.; Zamecnik, P.C. Rapid noninvasive detection of experimental atherosclerotic lesions with novel 99mTc-labeled diadenosine tetraphosphates. *Proc. Natl. Acad. Sci. U S A*., **1998,** *95*, 691-5.

110. Bauer, C.; Bauder-Wuest, U.; Mier, W.; Haberkorn, U.; Eisenhut, M. 131I-labeled peptides as caspase substrates for apoptosis imaging. *J. Nucl. Med*., **2005,** *46*, 1066-74.

111. Aloya, R.; Shirvan, A.; Grimberg, H.; Reshef, A.; Levin, G.; Kidron, D.; Cohen, A.; Ziv, I. Molecular imaging of cell death in vivo by a novel small molecule probe. *Apoptosis*., **2006,** *11*, 2089-101.

112. Faust, A; Wagner, S; Law, M.P.; Hermann, S; Schnöckel, U.; Keul, P.; Schober, O.; Schäfers, M.; Levkau, B.; Kopka, K. The nonpeptidyl caspase binding radioligand (S)-1-(4-(2-[18F]Fluoroethoxy)-benzyl)-5-[1-(2-methoxymethylpyrrolidinyl)sulfonyl]isatin ([18F]CbR) as potential positron emission tomography-compatible apoptosis imaging agent. *Q. J. Nucl. Med. Mol. Imaging*., **2007,** *51*, 67-73.

113. Luo, Q.Y.; Wang, F.; Zhang, Z.Y.; Zhang, Y.; Lu, H.K.; Sun, S.H.; Zhu, R.S. Preparation and bioevaluation of (99m)Tc-HYNIC-annexin B1 as a novel radioligand for apoptosis imaging. *Apoptosis*., **2008,** *13*, 600-8.

114. Dinkelborg, L.M.; Duda, S.H.; Hanke, H.; Tepe, G.; Hilger, C.S.; Semmler, W. Molecular imaging of atherosclerosis using a technetium-99m-labeled endothelin derivative. *J. Nucl. Med.*, **1998,** *39*, 1819-22.

115. Tepe, G.; Duda, S.H.; Meding, J.; Brehme, U.; Ritter, J.; Hanke, H.; Hilger, C.S.; Claussen, C.D.; Dinkelborg, L.M. Tc-99m-labeled endothelin derivative for imaging of experimentally induced atherosclerosis. *Atherosclerosis.*, **2001,** *157*, 383-92.

116. Meding, J.; Dinkelborg, L.M.; Grieshaber, M.K.; Semmler, W. Targeting of endothelin receptors for molecular imaging of atherosclerosis in rabbits. *J. Nucl. Med.*, **2002,** *43*, 400-5.

117. Sadeghi, M.M.; Krassilnikova, S.; Zhang, J.; Gharaei, A.A.; Fassaei, H.R.; Esmailzadeh, L.; Kooshkabadi, A.; Edwards, S.; Yalamanchili, P.; Harris, T.D.; Sinusas, A.J.; Zaret, B.L.; Bender, J.R.. Detection of injury-induced vascular remodeling by targeting activated alphavbeta3 integrin in vivo. *Circulation.*, **2004,** *110*, 84-90.

118. Matter, C.M.; Schuler, P.K.; Alessi, P.; Meier, P.; Ricci, R.; Zhang, D.; Halin, C.; Castellani, P.; Zardi, L.; Hofer, C.K.; Montani, M.; Neri, D.; Lüscher, T.F. Molecular imaging of atherosclerotic plaques using a human antibody against the extra-domain B of fibronectin. *Circ. Res.*, **2004,** *95*, 1225-33.

119. von Lukowicz, T.; Silacci, M.; Wyss M.T.; Trachsel, E.; Lohmann, C.; Buck, A.; Lüscher, T.F.; Neri, D.; Matter, C.M. Human antibody against C domain of tenascin-C visualizes murine atherosclerotic plaques ex vivo. *J. Nucl. Med.*, **2007,** *48*, 582-7.

120. Thurberg, BL; Collins, T. The nuclear factor-kappa B/inhibitor of kappa B autoregulatory system and atherosclerosis. *Curr. Opin. Lipidol.*, **1998**, *9*, 387–96.

121. De Nigris, F.; Lerman, L.O.; Rodriguez-Porcel, M.; De Montis, M.P.; Lerman, A.; Napoli C. C-myc activation in early coronary lesions in experimental hypercholesterolemia. *Biochem. Biophys. Res. Commun.,* **2001,** *281*, 945–50.

122. Qin, G.; Zhang, Y.; Cao, W; An, R.; Gao, Z.; Li, G.; Xu, W.; Zhang, K.; Li, S. Molecular imaging of atherosclerotic plaques with technetium-99m-labelled antisense oligonucleotides. *Eur. J. Nucl. Med. Mol. Imaging*., **2005**, *32*, 6–14.

123. Scanlon, K.J.Anti-genes: siRNA, ribozymes and antisense.*Curr. Pharm. Biotechnol.,* **2004**, 5, 415-20.

124. Blankenberg, F.G.; Strauss, H.W. Nuclear medicine applications in molecular imaging: 2007 update. *Q. J. Nucl. Med. Mol. Imaging*., **2007,** *51*, 99-110.